



INTERNATIONAL
YEAR OF LIGHT
2015

한국광학회 2014년도 하계학술발표회

Final Program of the Optical Society of Korea Summer Meeting 2014

프 로 그 램



일시 : 2014년 8월 25일(월) ~ 27일(수)

장소 : 제 주 국 제 컨 벤 션 센 터

주최 : 한 국 광 학 회

후원 : 한 국 과 학 기 술 단 체 총 연 합 회

2014. 8. 26 (화)

광자기술 I (T3B-V)

17:00~18:30 / 201B

좌장: 임영안(ETRI)

17:00(초청논문)

T3B-V 1 단일모드발진과 공진 방향 제어가 가능한 사각형 미소 공진기에 대한 연구

현경숙, 이진웅, 김대진, 정상혁(세종대)

We report a single mode lasing and an unidirectional operation of semiconductor double square ring resonators. The advantages of square ring resonator will be discussed.

17:30

T3B-V 2 실리콘 링 모듈레이터의 Self-Heating 모델링

반유진, 임진수, 유병민, 성연수, 이정민, 최우영(연세대)

We present a self-heating model for a Si micro-ring modulator. Our model is based on the coupled-mode theory. The accuracy of the model is confirmed with measurement.

17:45(초청논문)

T3B-V 3 파장 훑음 레이저와 이를 이용한 광섬유 센서

진민용, 고명욱, 최병권, 권용석(충남대)

In this presentation, I will review the several applications of the wavelength-swept lasers, which are used in dynamic fiber-optic sensors.

18:15

T3B-V 4 편광회전 반사간섭계를 이용한 광전압센서

추우성, 허성욱, 오민철(부산대)

An optical voltage sensors based on polarization rotated reflection interferometry is implemented by using a Lithium Tantalate (z-cut) crystal and polymeric optical integrated circuits (ICs).

광기술 II: 광기술 응용 (T3C-II)

17:00~18:30 / 202A

좌장: 김지현(경북대)

17:00(초청논문)

T3C-II 1 고효율 1064nm 레이저용 고성능 광학표면 형성 기술

김종섭(KOPTI)

고출력 레이저용 광학부품의 광학손실과 레이저 손상문턱치 성능을 향상시키기 위해서 세정, 에칭, 연마, 코팅 및 측정 등 전 과정에 대한 공정 최적화를 수행하였다. 이 중 광학적 초저손실 성능 구현을 위해서 광학표면 조도 향상, 면하손상 저감, 표면 결점 방지, 이물질 및 오염 제거 및 박막성능 최적화를 수행하였고, 또한 레이저 손상문턱치 성능 향상을 위해서 박막구조, 열적 특성, 스트레스, 열처리 최적화 및 청정환경 구현을 수행하였다.

17:30

T3C-II 2 정렬된 마이크로스피어 필름의 구조분석을 위한 편광현미경의 효율적 이용방법

김준현, 박정수, 김서향(APRI)

Polarized microscopy can be very effective in the inspection of the close-packed microsphere film. It gives a better contrast in identifying domain boundaries and the number of layers, compared to the other microscopic modes.

17:45

T3C-II 3 물포나비 생체모방구조에서 무질서도가 넓은 반사각에 미치는 효과

송보광, 엄석찬, 신중훈(KAIST)

From bio-mimetic structures inspired by Morpho butterfly wings, we have investigated the effect of nanoscale disorder among the multilayered ridges on broad-angle reflection.

18:00

T3C-II 4 반사형 코노스코픽을 이용한 물체의 깊이 정보 측정과 경향성 분석에 관한 연구

임상희, 김진환, 김재순(명지대), 정상호, 이동우(솔브레이니엔지)

본 연구는 반사형 코노스코픽 홀로그램을 구현하여 물체에 대한 깊이 정보를 interference fringe로부터 역 추산하였으며, 물체의 깊이 정보에 대한 경향성을 분석하였다.

18:15

T3C-II 5 도플러 OCT를 이용한 생체 내 중이의 진동 검출

전덕민, 조남현, 장정훈, 김지현(경북대)

Doppler Optical Coherence Tomography can offer 2-dimensional in real time tomogram of rapidly oscillatory mouse tympanic membrane and ossicular chain *in vivo*.

디지털홀로그래피 및 정보광학 III: 3D Display II (T3D-III)

17:00~18:30 / 202B

좌장: 최희진(세종대)

17:00(초청논문)

T3D-III 1 3D 영상 표시장치의 평가

홍형기(서울과학기술대)

3D 영상 기술은 3D 영화의 성공과 함께 급속히 활성화되었고, 이와 함께 3D 기술의 특성의 평가 및 표준화 활동도 활발하게 진행 중이다. 3D display에서 좌안과 우안에서의 휘도는 휘도계로 측정이 가능하나 좌안, 우안의 상이 융합되어 입체 영상으로 인지된 결과는 측정할 수 없다는 점에서 2D와 3D display의 측정에 차이가 있다.

17:30

T3D-III 2 Dot sampling 기법을 이용한 공간 분할 방식 지향성 백라이트 시스템의 인지 해상도 개선

박민영, 최희진(세종대)

In this paper, we will suggest a method to improve the perceived resolution of an autostereoscopic 3D display using spatial interlacing directional backlight system by adopting dot sampling technique.

17:45

T3D-III 3 무안경식 입체 디스플레이에서의 굴절률 효과에 관한 연구

윤선규, 김현우(KIST, 고려대), 김성원, 김성규(KIST)

The viewing zone is formed by optical plate, such as parallax barrier in the autostereoscopic display and was verified by using simulation the effect due to the refractive index of the optical plate.

18:00

T3D-III 4 3차원 영상 회의를 위하여 영상 획득 시스템과 광학적으로 등가 구조를 가지는 다시점 디스플레이

임성진, 정재혁, 윤지섭, 홍종우, 전준호, 성종민, 김성민, 한준구(경북대)

We present a multi-view display for 3D teleconference. This consists of plural projectors and retro-reflective screen and it is optically equivalent to the multi-view acquisition system.

Modeling of Si Micro-Ring Modulator Self-Heating

Yoojin Ban, Jinsoo Rhim, Byung-min Yu, Yunsu Sung, Jeong-min Lee and Woo-Young Choi*

Department of Electrical and Electronic Engineering, Yonsei University

*wchoi@yonsei.ac.kr

Si photonics has a great potential for realizing cost-effective, high-bandwidth, and small-footprint optical interconnect systems⁽¹⁻²⁾. The Si electro-optic modulator is one of the key components for Si photonic optical interconnect systems. In particular, a Si micro-ring modulator (Si MRM) is attracting a great amount of research interests as it can provide large bandwidth and high modulation efficiency with a small size and low power consumption⁽³⁾. An accurate model for the Si MRM is necessary for designing transmitters for optical interconnect applications. There are several dynamic models of Si MRM⁽⁴⁻⁵⁾. However, there is no Si MRM model that can include the self-heating effect. In this paper, we present a model based on the coupled-mode theory that includes self-heating of the Si MRM due to free carrier absorption (FCA). In addition, we confirm the accuracy of our model with measurement.

Figure 1 shows the structure of the Si MRM used for our investigation. Input light passing through the bus waveguide is partially coupled into the ring waveguide. Circulating light in the ring waveguide experiences phase shifts. Then, a portion of circulating light couples out to the bus waveguide and interferes with the uncoupled input light. Round-trip phase shifts are electrically tunable with an embedded reverse biased PN junction, which enables high speed operation. The figure also includes a microphotograph of the fabricated Si MRM. It is fabricated on 220-nm thick Si layer on 2- μm buried oxide layer through the OpSIS-IME multi-project-wafer foundry service.

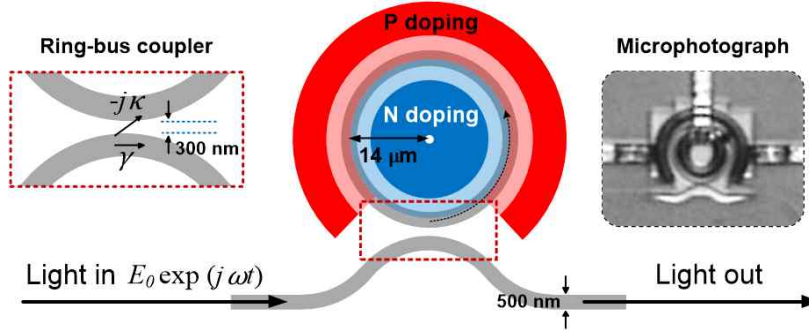


Fig. 1. Structure and microphotograph of the Si micro-ring modulator.

From the coupled-mode theory, Si MRM dynamics can be modeled as⁽⁶⁾

$$\frac{da(t)}{dt} = (j\omega_0 - 1/\tau)a(t) - j\mu E^i(t) \quad \text{and} \quad E^t(t) = E^i(t) - j\mu a(t). \quad (1)$$

In the above equation, $a(t)$ represents a total energy amplitude stored in the ring with resonance angular frequency ω_0 . ω_0 is given as $2\pi mc/(\eta_0 L)$ with the mode number m , the speed of light c , the group index of the ring η_0 , and the ring circumference L . $E^i(t)$ and $E^t(t)$ represent input and output optical field, respectively, where E^i is given as $E_0 \exp(j\omega t)$. τ is the decay time constant satisfying $1/\tau = (1 - \alpha^2 + \kappa^2)c/(2\eta_0 L)$, where a represents the round-trip loss and κ is the coupling coefficient for the ring-bus coupler. μ is the mutual coupling coefficient satisfying $\mu^2 = \kappa^2 c/(\eta_0 L)$.

Since the optical power can be highly concentrated in the ring, thermal resonance shift due to two photon absorption (TPA) or FCA can be observed with high input power. In Si MRM with PN junction, it has been found that FCA is the dominant factor for thermal resonant shift⁽⁷⁾. Generated heat through FCA in the doped ring waveguide increases the refractive index of the waveguide. This becomes more pronounced closer to the resonance due to the higher optical power density, resulting in the skewed resonance peak. Group index of the ring n_0 can be modeled as a function of $|A(t)|^2$, the total optical power in a cross section of the ring waveguide as

$$\eta(t) = \eta_0 + \sigma |A(t)|^2 = \eta_0 + \sigma |a(t)|^2 / T, \quad (2)$$

where σ is a refractive index change coefficient and T is the round-trip time.

Eq. (1) can be numerically calculated with changing n_0 in each time step. Figure 2(a) shows the measured transmission curves with different input optical powers as well as the calculated results obtained from Eq. (1). Extracted ring parameters from fitting the transmission curve at -10 dBm input power are $a=0.940$ and $k=0.235$. Refractive index change coefficient σ is extracted as $7.8 \times 10^{-5} \text{ mW}^{-1}$. Figure 2(b) shows the resonance wavelength shift which linearly depends on the ring input power.

In summary, we successfully modeled the self-heating effects of the Si MRM using the coupled-mode theory. Values for the refractive index change coefficient and ring parameters are extracted with measurement results. Simulations and measurements are in good agreement.

5 dBm
0 dBm
-5 dBm
-10 dBm

Fig. 2. (a) Transmission curves with different levels of input laser power. (b) Resonance wavelength shift as a function of ring input power.

References

1. R. Soref, IEEE J. Sel. Top. Quantum Electron. **12**(6), 1678-1687 (2006).
2. Q. Xu, et al, Nature **435**, 325-327 (2005).
3. P. Dong, et al, Opt. Express **17**(25), 22484-22490 (2009).
4. W. D. Sacher and J. K. S. Poon, Opt. Express **16**(20), 15741-15753 (2008).
5. M. Song, et al, IEEE J. Sel. Top. Quantum Electron. **16**(1), 185-191 (2010).
6. B. E. Little, et al, J. Lightwave Technol. **15**, 998-1005 (1997).
7. X. Zheng, et al, Opt. Express **20**(10), 11478-11486 (2012).